JOURNAL OF MATERIALS SCIENCE 24 (1989) 3616–3620

Fatigue behaviour characterization of the fibre–matrix interface

R. A. LATOUR Jr, J. BLACK
McKay Laboratory of Orthopaedic Surgery Research, Univeristy of Pennsylvania, Philadelphia, Pennsylvania 19104, USA

B. MILLER
Textile Research Institute, Princeton, New Jersey 08542, USA

The fracture behaviour of FRP composite materials is significantly influenced by the behaviour of the fibre–matrix interfacial bond. Thus far interfacial bond mechanical characterization has been based upon the critical strength and critical fracture energy of debonding. Characterization of the fatigue behaviour of the interfacial debonding process, however, may be more valuable for composite design and fibre–matrix selection. A fracture mechanics model of interfacial bond fatigue based on the mode II strain energy release rate (G_{II}) is presented. An expression for G_{II} is derived for a single fibre in matrix cylinder model. By fitting the model to single fibre pull-out fatigue test data, fatigue crack propagation plots for specific fibre–matrix combinations can be drawn. These should prove useful for the development of fatigue resistant FRP composite materials.

1. Introduction

The structural failure of FRP materials involves three types of local failure: fibre fracture, matrix fracture, and fibre–matrix interfacial bond fracture. While the properties of the fibre and matrix are obviously important governing factors of the failure process, it is the interfacial bond behaviour which ultimately determines the synergism of fibre and matrix properties as they blend together to produce composite behaviour. Investigations of fracture phenomena of FRP composite materials have demonstrated that interface behaviour affects composite stiffness [1, 2], strength [3, 4], toughness [3, 4], fatigue resistance [5], and environmental stability [6–8]. The importance of interfacial bond behaviour is summed up by Drzal [7] who concludes that "the exact nature of this region (interfacial bond region) must be understood if accurate life prediction models (of composite behaviour) are to be developed".

2. Interfacial bond characterization

Two main approaches towards interfacial bond characterization have been taken: The first has been to determine the ultimate shear strength (critical stress) of the interfacial bond [4, 7, 9, 10] and the second, to determine the amount of energy per unit area required to cause unstable or rapid shear crack growth [11–13]. The later, or critical energy method, is based upon measuring the mode II critical strain energy release rate (G_{IIc}) which is related to the energy of fracture [11, 14].

While critical stress and critical energy methods of interfacial bond characterization contribute significantly to the understanding of the failure processes involved in interfacial debonding, they are based upon quasi-static (single cycle loading to failure) tests as opposed to fatigue tests.

In a study related to interfacial bond fatigue, Mall and Johnson [15] observed that significant debonding occurs in adhesively bonded lap joints cyclically loaded at strain energy release rates an order of magnitude below their critical strain energy release rate values. The fibre–matrix interface may well show a similar fatigue behaviour. Very little work, however, has yet been done in this area. Apparently only one report has been published on the application of this approach to interfacial debonding in FRP composite materials. In this study, Gradin and Backlund [16] performed interfacial bond fatigue tests on a 1 cm diameter steel rod "potted" in transparent epoxy as a macroscopic representation of a single fibre embedded in a plastic matrix. With this model, Gradin and Backlund did observe a slow crack growth debonding process. This suggests that interfacial debonding in FRP composites does follow a cumulative fracture, or fatigue failure process. If this is true, then interfacial bond characterizations based upon interfacial bond fatigue behaviour should be used for the design of fatigue resistant FRP composite materials rather than those that are based upon critical interfacial properties (stress or energy).

In the light of this, an investigation was undertaken to determine if fatigue crack propagation does occur for actual scale fibre–matrix interfacial bonds (as opposed to macro-models [16]), and if so, to characterize this fatigue process. We have selected a microdroplet single-fibre pull-out test model previously used for quasi-static (single cycle) tests [10] for our fatigue test model. This model involves the embedment of very short fibre lengths (about 100 μm) within microdroplets of polymer matrix to form fibre pull-out test specimens. The interface is tested in fatigue by supporting the microdroplet in a grip while a sinusoidal

0022–2461/89 $03.00 + .12

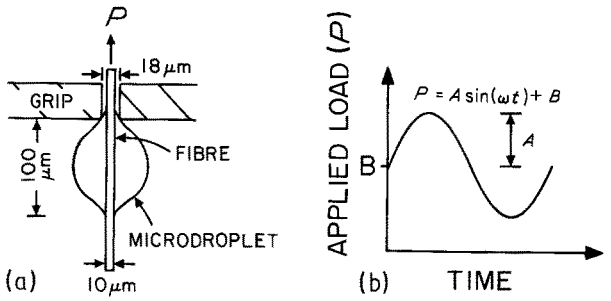

Figure 1 Sample model for interfacial bond fatigue testing. (a) Fibre/microdroplet in grip. (b) Fatigue load programme applied to fibre.

subcritical controlled load is applied to the fibre (Fig. 1). The number of cycles applied is recorded on a cycle counter. The interface fatigues until the residual bond between the microdroplet and fibre can no longer support the peak applied load, at which point abrupt complete debonding and fibre pull-out occurs. This method permits interfacial bond fatigue data to be obtained in the form of applied peak load against number of cycles to failure plots (S–N fatigue plot). To characterize the fatigue process, fatigue constants c and m of the fracture mechanics expression $da/dN = cG_{II}^m$ may be determined from the test data (da/dN = crack growth per load cycle).

A miniature closed-loop fatigue testing machine for the application of controlled cyclic loading has been designed and constructed for use in this investigation (patent granted, to issue) and fatigue testing is presently underway. Preliminary test results using fibre–thermoplastic specimens indicate that the interface does fatigue under subcritical loading. An interfacial bond fatigue S–N plot obtained for polyaramid fibre–polycarbonate matrix specimens is presented in Fig. 2 as an example of our preliminary data. In this paper we present a mathematical model which is appropriate for analysis of interfacial bond fatigue data resulting from such tests.

3. Mathematical model of interfacial bond fatigue

In order to model the interfacial bond fatigue behaviour in the form

$$\frac{da}{dN} = cG_{II}^m \qquad (1)$$

an expression for G_{II} must be derived for the model

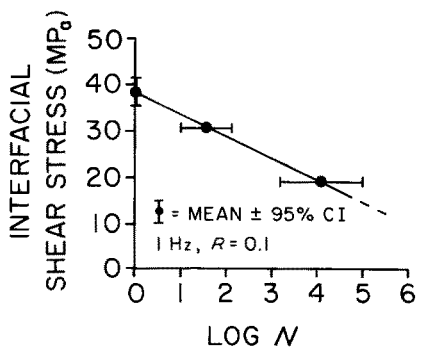

Figure 2 Interfacial bond fatigue plot for polyaramid fibre–polycarbonate matrix microdroplet samples. (Interfacial shear stress = pull-out force ÷ interfacial bond area.)

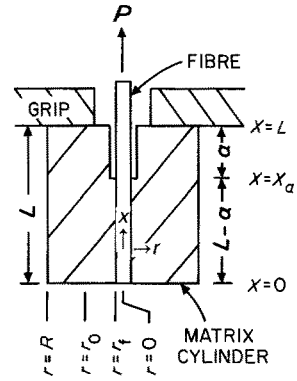

Figure 3 Cylindrical model representation of fibre–microdroplet sample.

system. G_{II} can be expressed in terms of the change in material compliance per change in crack area [17]

$$G_{II} = \frac{p^2}{2}\frac{d(u/p)}{dA} \qquad (2)$$

where G_{II} is the mode II strain energy release rate, p is the constant applied load, (u/p) is the material compliance (displacement ÷ applied load), and A is one half of the total surface area of the crack [17, 18].

3.1. Derivation of G_{II} for the sample model

Our sample model may be represented as a single uniaxial fibre embedded in a cylinder of matrix (Fig. 3). The matrix cylinder is supported at its base while load p is applied to the fibre. $(L\text{-}a)$ represents the bonded length and a the debonded length of the fibre along the interface. For our mathematical treatment of this model, the cylinder is broken up into two subdivisions (Fig. 4). The first (Fig. 4a) represents the debonded fibre and matrix between $X = X_a$ and $X = L$. Here, the matrix is assumed to be under uniform compression (σ_m) and the fibre under uniform tension (σ_f). The second (Fig. 4b) represents the interfacially bonded segment of the model. Here it is assumed that the stress field local to the fibre (Fig. 3: from $r = r_f$ to $r = r_0$, where r_0 is not specified) is that of pure shear ($\tau_{rx} = \tau(x, r)$, $\sigma_x = \tau_{r\theta} = 0$). With these assumptions, force equilibrium in the x direction results in the relationship of

$$r\tau_{rx} = \text{constant} \qquad (3)$$

This stress field approximation is commonly used in single fibre composite models to represent the shear stress field surrounding a fibre [19, 20]. At $r = r_0$ the matrix is assumed to have negligible displacement in the x direction ($u_x \approx 0$).

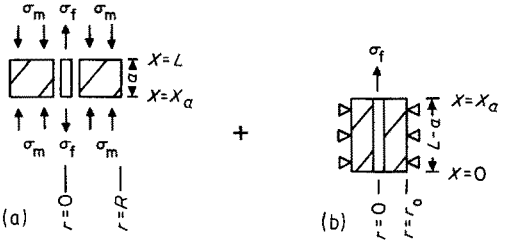

Figure 4 Subdivisions of fibre–matrix cylinder for the mathematical model. (a) Model representation of debonded interface segment. (b) Model representation of bonded interface segment.

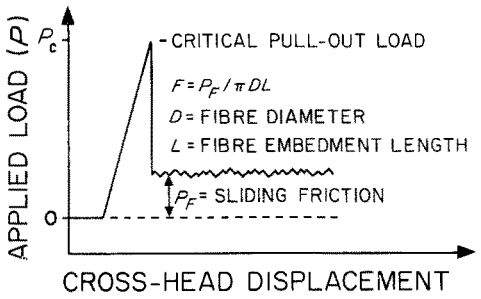

Figure 5 Determination of interface frictional shear stress (F) from single-cycle fibre pull-out x–y recorder trace.

3.2. Compliance

The compliance (u/p) of this model can be subdivided into three separate compliance contributions: fibre, matrix, and interface

$$(u/p)_{\text{total}} = (u/p)_{\text{fibre}} + (u/p)_{\text{matrix}} + (u/p)_{\text{interface}} \quad (4)$$

where the fibre and matrix compliance contributions account for the compliance of the debonded segment (Fig. 4a) and the interface compliance accounts for the compliance of the bonded segment (Fig. 4b).

3.2.1. Fibre compliance

Given an applied tensile load, p, and an interface frictional shear stress, F, along the debonded segment of the fibre, the fibre tensile stress, σ_f, is given by

$$\sigma_f = \frac{p - 2\pi r_f F(L - X)}{\pi r_f^2} = E_f \frac{du}{dX} \quad (5)$$

Rearranging and integrating to obtain the fibre compliance

$$(u/p)_f = \frac{1}{\pi r_f^2 E_f p}(pa - \pi r_f F a^2) \quad (6)$$

where F (force/area) represents the frictional stress between the debonded fibre and the matrix (F is determined by single cycle pull-out test (Fig. 5) [10]), L = fibre embedment length, σ_f = fibre tensile stress, r_f = fibre radius, E_f = fibre modulus, $a = L - X$ = interfacial crack length, and du/dX = differential displacement per differential length in the x direction.

3.2.2. Matrix compliance

Assuming that the matrix surrounding the debonded section of the fibre deforms as a cylinder under uniform compression, and taking into account interfacial friction, the matrix stress, σ_m, is given by

$$\sigma_m = \frac{p - 2\pi r_f F(L - X)}{A_m} = E_m \frac{du}{dX} \quad (7)$$

Rearranging and integrating to obtain the matrix compliance

$$(u/p)_m = \frac{1}{E_m A_m p}(pa - \pi r_f F a^2) \quad (8)$$

where σ_m is the matrix compressive stress, E_m the matrix modulus, A_m the cross-sectional area of matrix = $\pi(R^2 - r_f^2)$, and $(du/dX)_m$ the differential displacement per differential length in the x direction.

3.2.3. Interfacial bond compliance

The displacement of the interface per applied load is the sum of two displacements: (1) the displacement, u_1, due to the fibre tensile stress along its bonded length, and (2) the displacement, u_0, of the fibre end at $X = 0$.

Values for u_1 and u_0 are calculated from the expressions for fibre tensile stress and interfacial shear stress for the model by the "shear-lag" method [9, 21] of interfacial stress analysis. Again, frictional load transfer over the debonded fibre length is accounted for. Fibre tensile stress (σ_f) and interfacial shear stress (τ_i) are given by

$$\sigma_f = \frac{p - 2\pi r_f F a}{\pi r_f^2} \frac{\sinh(\beta X/r_f)}{\sinh(\beta X_a/r_f)},$$

where

$$\beta^2 = \frac{2G_m}{E_f \ln(r_0/r_f)} \quad (9)$$

$$\tau_i = \frac{\beta(p - 2\pi r_f F a)}{2\pi r_f^2} \frac{\cosh(\beta X/r_f)}{\sinh(\beta X_a/r_f)} \quad (10)$$

where β is a geometric and mechanical property parameter which must be determined experimentally by fitting Equation 10 to single-cycle pull-out test results.

The compliance contribution from u_1 is therefore

$$(u/p)_1 = \frac{p - 2\pi r_f F a}{\pi r_f E_f p \beta} \frac{\cosh[\beta(L - a)/r_f] - 1}{\sinh[\beta(L - a)/r_f]} \quad (\text{with } X_a = L - a) \quad (11)$$

To develop a compliance expression for $(u/p)_0$ a shear stress equilibrium of $r\tau = r_f \tau_i$ (see Equation 2) is assumed. Following integration of this stress field from $r = r_f$ to $r = r_0$ at $x = 0$ the compliance contribution is obtained

$$(u/p)_0 = \frac{p - 2\pi r_f F a}{\pi r_f E_f p \beta} \frac{1}{\sinh(\beta X_a/r_f)} \quad (12)$$

3.3. Total system compliance

The total system compliance is the sum of the four component compliances (4) = (6) + (8) + (11) + (12)

$$(u/p)_t = \left(a - \frac{\pi r_f F a^2}{p}\right)\left(\frac{1}{E_m A_m} + \frac{1}{E_f \pi r_f^2}\right) + \frac{[p - (2\pi r_f F a)] \coth[\beta(L - a)/r_f]}{p \pi r_f E_f \beta} \quad (13)$$

3.4. Strain energy release rate

The strain energy release rate for the fibre–matrix model can now be expressed as a function of the crack length a

$$G_{II} = \frac{p^2}{2} \frac{d(u/p)}{dA} = \frac{p^2}{4\pi r_f} \frac{d(u/p)}{da} \quad (14)$$

By substitution of Equation 13 into Equation 14

$$G_{II} = \frac{(p^2 - 2\pi r_f Fpa}{4\pi r_f}\left\{\frac{\coth^2[\beta(L-a)/r_f]}{\pi r_f^2 E_f} + \frac{1}{E_m A_m}\right\} - \frac{Fp\coth[\beta(L-a)/r_f]}{2\pi r_f \beta E_f} \quad (15)$$

3.5. Determination of fracture mechanics parameters

The expression for the strain energy release rate (Equation 15) can now be substituted into Equation 1 to yield a description of the fatigue behaviour of the single fibre in matrix cylinder model. For the sake of simplicity G_{II} is represented here as a function of a, p, and F [$G_{II} = G(a, p, F)$]

$$\frac{da}{dN} = cG(a, p, F)^m \quad (16)$$

This expression can be integrated and rearranged to obtain

$$N_c = \frac{1}{c}\int_0^{a_c} G(a, p, F)^{-m}\, da \quad (17)$$

where N_c is the total number of fatigue cycles applied to the sample to cause fibre pull-out and a_c represents the distance an interfacial crack will grow before the bond strength (or energy) reaches its critical level for unstable crack propagation. When a_c is reached (at $N = N_c$) complete debonding will occur. The value of a_c can be calculated using Equation 10 by letting $X = X_a = L - a$, p = peak applied load and τ_i = critical interfacial shear stress (determined by single fibre pull-out test [10]), and then solving for a.

Equation 17 may be fitted to experimental fatigue data to determine the value of fatigue constants c and m for each fibre–matrix combination tested. This may be done by evaluating $G(a, p, F)$ (Equation 15) at two different load levels: p_1 and p_2. Each of these expressions may be separately substituted into Equation 17 along with the corresponding calculated critical crack length (a_{c1} or a_{c2}) and experimentally determined number of cycles to failure (N_{c1} or N_{c2}). This results in two independent equations with two unknowns (c and m) which can be simultaneously solved to determine the value of c and m. Once these constants are determined, interfacial bond fatigue diagrams for each material system can be constructed in the form of plots of da/dN against $G(a, p, F)$ or a against N for a specified applied peak load condition.

4. Discussion

A mathematical model has been developed to describe interfacial bond fatigue for a single axially loaded fibre within a matrix cylinder. This model is based upon a fracture mechanics expression which relates fatigue crack propagation to G_{II}. An expression for G_{II} has been developed for the single fibre model as the sum of the individual strain energy release rate contributions of the fibre, matrix, and interface. Others who have used this method to derive an expression for the critical strain energy release rate (G_{IIc}) have reported G_{IIc} to be a function of the fibre contribution alone [11, 12, 22]. These studies, however, have all involved the pull-out of long fibre embedment lengths from relatively large blocks of matrix. For the case of very short embedment lengths of fibre within a small base supported matrix cylinder, all three contributions (fibre, matrix, and interface) are necessary. This is the case for the microdroplet sample model. It can be seen from Equation 15 that as L/r_f and A_m increase, G_{II} tends toward a value equal to that which would be obtained if only the fibre contribution (Equation 6) where considered (e.g. matrix and interface contributions become negligible as L/r_f and A_m become large). Thus, the expression for G_{II} given in Equation 15 is in agreement with the literature.

Several difficulties arise from the application of this mathematical model to the analysis of fatigue data generated by the microdroplet sample model. First, a microdroplet is in the shape of a double tear-drop (Fig. 1) while the analysis assumes that it is a cylinder of outer radius equal to an average cross-sectional radius of the microdroplet. Secondly, the necessity of supporting a microdroplet at its base very close to the fibre raises the question of grip effects. Thirdly, the crack front is not recognizable in the droplet during testing, possibly because of the sample's microscopic size, and therefore must be calculated. It is also possible that, in the microdroplet model, the interface does not fail by a single slow crack propagation mechanism at all but rather by a general bond weakening (dispersed microcracking) process which occurs uniformly along the interface. In this case, the crack length (a) can be considered an analytical representation of the sum of all these microcracks as opposed to a single interfacial crack. Despite these complexities, preliminary test results with the microdroplet sample model do indicate that the interface undergoes fatigue and that the fatigue process is reproducible (Fig. 2). Therefore, even if the above problems do compromise the accuracy of this method for predicting actual debonding rates in multifibre FRP composite systems, the relative fatigue performance of fibre/matrix material combinations indicated by this sample model should still provide very useful guideline information for composite design.

Values of fatigue constants c and m from Equation 16 may be determined by fitting the mathematical model to fatigue data. From these constants fatigue crack propagation diagrams may be plotted. Fatigue diagrams are often drawn in the form of Equation 16 (da/dN against G_{II}). For interfacial bond fatigue, however, this type of plot (Fig. 6a) could be misleading due to the effect of interfacial friction. According to Equation 15, interfacial friction decreases the crack growth driving force (G_{II}) as the crack length a increases. Therefore, while two fibre–matrix combinations may have identical plots of da/dN against G_{II} (e.g. equal values of fatigue constants c and m) they may differ considerably in their actual resistance to bond fatigue depending upon their relative levels of interfacial friction. For this reason, interfacial bond fatigue may be better represented by plotting actual crack length (instead of crack rate) against applied fatigue cycle (N) (Equation 17, with $N = N(a)$ instead of $N = N(a_c)$). Such plots (Fig. 6b) should prove

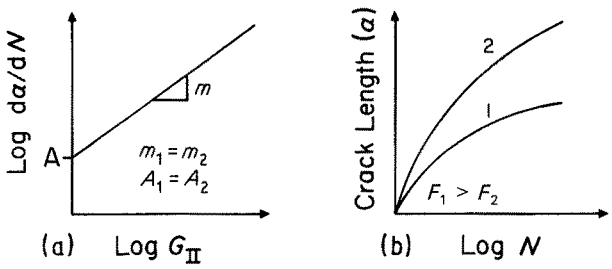

Figure 6 Interfacial bond fatigue characterization diagrams. (a) Hypothetical fatigue plot for materials 1 and 2. (b) Hypothetical plot of interface crack length, a, against load cycle, N, for materials 1 and 2.

very useful for the design of fatigue resistant FRP composite materials as they will provide a basis for fibre–matrix combination selection as well as information on the effects of design variables such as fibre aspect ratio, modulus, and volume fraction upon bond fatigue.

5. Conclusions

Interfacial debonding is an important governing factor of the fracture behaviour of FRP composites. Up until now, the primary emphasis for interfacial bond characterization has been the determination of the interfacial bond critical properties (strength or energy). This mode of characterization may not be sufficient, however, if significant interfacial debonding occurs with the application of loads (or strain energy levels) below these critical values.

Preliminary interfacial bond testing indicates that the fibre–matrix interface does experience fatigue under subcritical loading. Fatigue characterization of the interfacial debonding process is therefore necessary. A model is presented for the determination of fatigue constants based upon experimental data. Once these constants are determined, fatigue plots descriptive of the interfacial debonding process for specific fibre–matrix materials in specific test environments can be drawn. Such plots should provide very useful information for the design of fatigue resistant FRP composite materials.

Acknowledgement

We gratefully acknowledge the National Science Foundation for its support of this work (NSF grant ECE-8619897).

References

1. G. C. SHIH and L. J. EBERT, *Comp. Sci. Tech.* **28** (1987) 137.
2. P. S. STEIF, *J. Comp. Mater.* **17** (1984) 153.
3. A. TAKAKU and R. G. C. ARRIDGE, *J. Phys. D Appl. Phys.* **6** (1973) 2038.
4. M. J. FOLKES and W. K. WONG, *Polymer* **28** (1987) 1309.
5. J. A. MANSON, *Appl. Chem.* **57** (1985) 1667.
6. D. DEW-HUGHES and J. L. WAY, *Composites* **4** (1973) 167.
7. L. T. DRZAL, *Sampe. J.* **19** (1983) 7.
8. M. R. PIGGOTT, A. SANADI, P. S. CHUA and D. ANDISON, in "Composite Interfaces", edited by S. H. Ishida and J. L. Koenig (Elsevier, New York, 1986) p. 109.
9. P. S. CHUA and M. R. PIGGOTT, *Comp. Sci. Tech.* **22** (1985) 33.
10. B. MILLER, P. MURI and L. REBENFELD, *ibid.* **28** (1987) 17.
11. H. STANG, *Serie R-Dan. Tek. Hojsk. Afd. Baerende Konstr.* **205** (1985) 1.
12. H. STANG and S. P. SHAH, *J. Mater. Sci.* **21** (1986) 953.
13. C. ATKINSON, J. AVILA, E. BETZ and R. E. SMELSER, *J. Mech. Phys. Solids* **30** (1982) 97.
14. P. S. CHUA and M. R. PIGGOTT, *Comp. Sci. Tech.* **22** (1985) 107.
15. S. MALL and W. S. JOHNSON, in "Composite Materials: Testing and Design (7th Conf.)", ASTM STP 893 (American Society for Testing and Materials, Philadelphia, Pennsylvania, 1986) p. 322.
16. P. A. GRADIN and J. BACKLUND, in "Advances in Composite Materials", ICCM3, 3rd International Conference on Composite Materials, Vol. 1, edited by A. R. Bunsell, C. Bathias, A. Martrenchar, D. Menkes, and G. Verchery (Pergamon, New York, 1980) p. 162.
17. D. K. FELBECK and A. G. ATKINS, "Strength and Fracture of Engineering Solids" (Prentice-Hall, Englewood Cliffs, New Jersey, 1984) p. 332.
18. D. BROEK, "Elementary Engineering Fracture Mechanics", 3rd Revised Edn (Martinus Nijhoff, Boston, Massachusetts, 1982) p. 115.
19. P. LAWRENCE, *J. Mater. Sci.* **7** (1972) 1.
20. A. KELLY, "Strong Solids" (Oxford University Press, New York, 1966) p. 125.
21. M. R. PIGGOTT, *Comp. Sci. Tech.* **30** (1987) 295.
22. J. K. WELLS and P. W. R. BEAUMONT, *J. Mater. Sci.* **20** (1985) 1275.

Received 17 August 1988
and accepted 11 January 1989